Considerations on the influence of the current ripple and switching frequency towards the differential mode EMI filter

Andressa C. Schittler, Thiemo Kleeb, Mehmet Kazanbas, Samuel V. Araújo, Peter Zacharias
Center of Competence for Distributed Electric Power Technology (KDEE), University of Kassel
Wilhelmshöher Allee 71, 34121 Kassel, Germany
schittler@uni-kassel.de

Abstract

With new semiconductor technologies of outstanding performance each day more accessible, higher power density converters are being developed and introduced in the market, taking advantage of the potential increase on switching frequency offered by such devices without efficiency decrease. Attempting a further inductor size decrease, its value can be reduced, consequently increasing the current ripple up to trade-off between size and magnetic losses. However, the operation with higher switching frequency yields unusual EMI issues, as the higher magnitude harmonics (1st, 2nd, etc) of the generated noise to be attenuated are located close to or within the frequency range limited by current EMC standards. The current ripple also influences the harmonic content, increasing the noise amplitude. Therefore, based on a grid-connected full-bridge inverter, this paper presents an analysis towards the influences of the current ripple and switching frequency on the overall losses, minimization possibility and EMI filter design.

1 Introduction

In power converters design, some of the main goals are overall costs reduction, compactness and high efficiency.
Because of recent semiconductor developments, as improvements on Silicon-based switches and insertion of new technologies as Wide-Band Gap (WBG) technologies, the commutation frequency can be significantly increased without impact on the overall efficiency [1-3].
Magnetic components can have their volume and weight reduced by the switching frequency increase, consequently rising the power density of the converter.
Another step towards power filter inductor compaction would be to increase the current ripple through the inductors. Nevertheless, this strategy has two main drawbacks: first the magnetic losses increase, which may require extra cooling; second with higher current ripple, the output high frequency noise would be higher, possibly increasing the volume of the EMI filter, as well as the overall volume [4-5].
Regarding EMC compliance, for non-military applications, the majority of equipments are covered by CISPR11 standard (and similar standards) and foreseen limits for conducted emissions (CE) are between the 150 kHz to 30 MHz range.
As the switching frequency increases towards the CE standards frequency range, the highest amplitude harmonics multiple of the commutation frequency are placed near to or inside this range, leading to a more challenging design of the EMI filter.
This paper presents an analysis of the overall system volume reduction possibility according to the switching frequency and current ripple increase. A 100 kHz grid-connected full-bridge inverter with bipolar modulation has been tested in order to evaluate the switching frequency influence on the EMI and different filter topologies have been implemented, targeting to meet the standard compliance (Class B).
The noise source is described in Section 2 and the EMI filter design in Section 3. Overall losses (magnetics and semiconductors) are discussed in Section 4 and EMI measurements are presented in Section 5. Finally important points of discussion are highlighted, as well as the conclusion of the work presented.

2 Noise source description

A 2.3 kW grid-connected full-bridge inverter (Fig. 1) has been implemented with bipolar modulation in order to evaluate the switching frequency increase effects on the differential mode (DM) noise. The low high frequency (HF) common-mode (CM) noise is a clear advantage, besides the simple implementation.
Theoretical waveforms are shown in Fig. 2, depicting the output current together with the correspondent first harmonic (top) and the inductor current ripple (bottom). The ripple variation occurs due to the duty-cycle dependence of the output voltage, as (1).

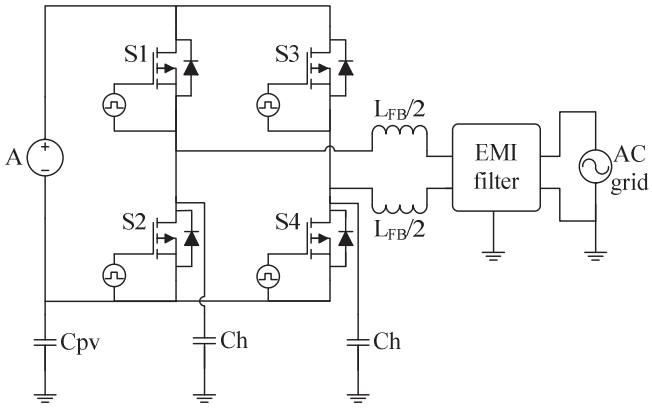

Figure 1 Full-bridge inverter

ISBN 978-3-8007-4171-7

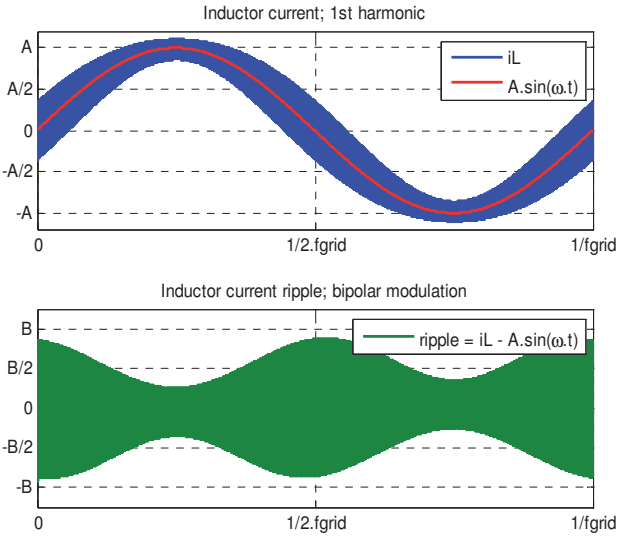

Figure 2 Top: theoretical current ripple with bipolar modulation and first harmonic; bottom: effective current ripple.

$$Dc(\theta) = \frac{ma.sin(\theta) + 1}{2} \qquad (1)$$

Where *ma* is the modulation index.

2.1 Differential mode noise

The DM noise source can be described as a current source placed between line and neutral (Fig. 3). Such noise has a triangular (filter inductor current - already 20 dB/dec attenuated) or a rectangular (full-bridge output current) waveform.

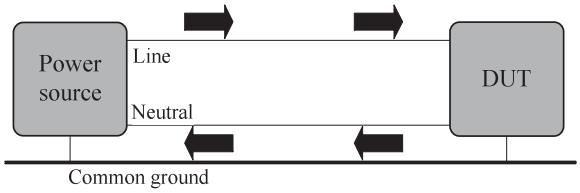

Figure 3 Differential mode noise representation.

2.2 Harmonic content

The Fourier amplitudes for a rectangular waveform can be calculated as (2), where the worst case scenario occurs for sin(x)=1.

$$A_h = \frac{4.A}{\pi} . \frac{\sin(h.Dc.\pi)}{h} . (-1)^h \qquad (2)$$

Where A is the amplitude of the DC input voltage and h is the harmonic order.

2.2.1 Influence of the switching frequency

For a rectangular waveform with variable duty-cycle, the respective harmonic content contains odd and even components. If only the switching frequency is changed, the amplitudes in the spectrum are kept constant, but are dislocated to meet the correspondent frequency multiples.

Figure 4 shows the harmonics for several switching frequencies. As it can be seen, the first harmonic from 100 kHz is outside the standard frequency range, which could be a design advantage, as the second harmonic is 6 dB lower.

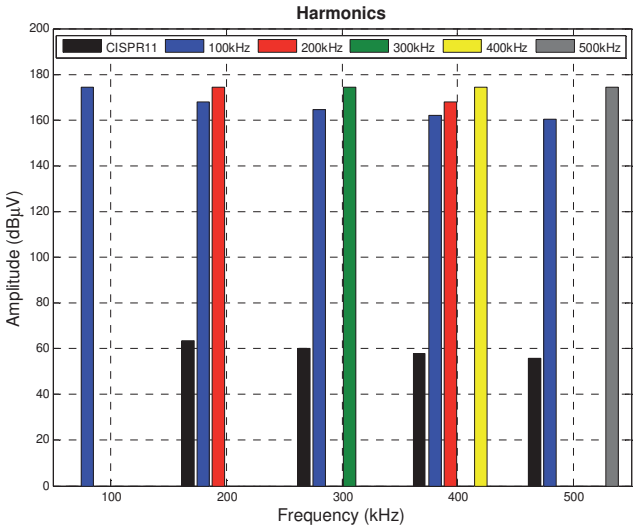

Figure 4 Emitted noise (dBµV) for different switching frequencies.

2.2.2 Influence of the input voltage

Even though it is possible to decrease the input voltage value as a way to reduce the harmonics amplitude, the variation of the first harmonic for the worst case scenario versus the input voltage in dBµV is shown at Figure 5. The voltage decrease from 500 V to 350 V leads to a 3dB decrease of the first harmonic amplitude.

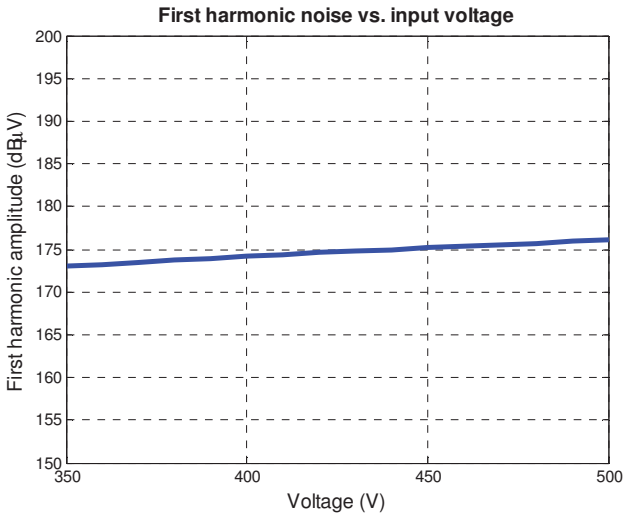

Figure 5 First harmonic amplitude (dBµV) versus input voltage (V).

3 Filter design

The EMI filter prediction has been performed according to simulations results (Matlab/PLECS), as the harmonics of interest are located at frequencies below 1 MHz.

ISBN 978-3-8007-4171-7

3.1 Power filter design

The power filter was designed according to the procedure shown in [6] being adapted to a full-bridge topology with bipolar modulation, as (3). The inductance values according to each switching frequency and RMS ripple are depicted in Figure 6, clearly pointing to a maximum value if both ripple and switching frequency are low.

$$L_{FB} = \frac{A}{4.f_{sw}.f_{grid}.I_R}\sqrt{\frac{1}{3}.\left(1 - ma^2 + \frac{3}{8}.ma^4\right)} \quad (3)$$

Where *fsw* is the switching frequency,
fgrid is the grid frequency (50 Hz),
I_R is the RMS ripple

3.2 EMI filter design

A simple LC filter structure with two stages was investigated, however similar trends can also be expected for π filter structures. Both, inductors and capacitors were designed according to the method presented in [6], based on the transfer matrix A and coefficient K, as shown in (4) and (5).

$$L = \frac{Ro}{2.\pi.F_O} \quad (4)$$

$$C = \frac{1}{4.\pi^2.{F_O}^2.L} \quad (5)$$

Where *Ro* is the base resistance (50 Ω) and
Fo is the cut-off frequency, based on the K value.

Figure 7 and Figure 8 show the results for the designed EMI filter, for inductors and capacitors. A step can be seen at 150 kHz, meaning the beginning of the EMI standard CISPR11. The capacitance plot is discrete because it is based on manufacturer values for Film capacitors.
Figure 9 shows the sum from all inductances in order to illustrate the overall inductance of the magnetic components. Regarding the inductances, it is already possible to recognize very low inductance values around 400 kHz and 20%-25% RMS ripple. From 350 kHz up to 500 kHz an almost constant value for every current ripple, meaning that the minimization has reached a limit. Such limit will be defined by switching losses as well as by the magnetic components performance.

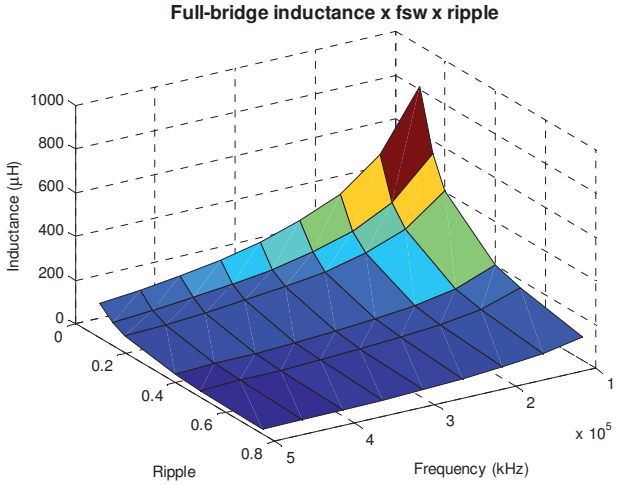

Figure 6 Power filter inductance (µH) versus ripple and switching frequency (kHz)

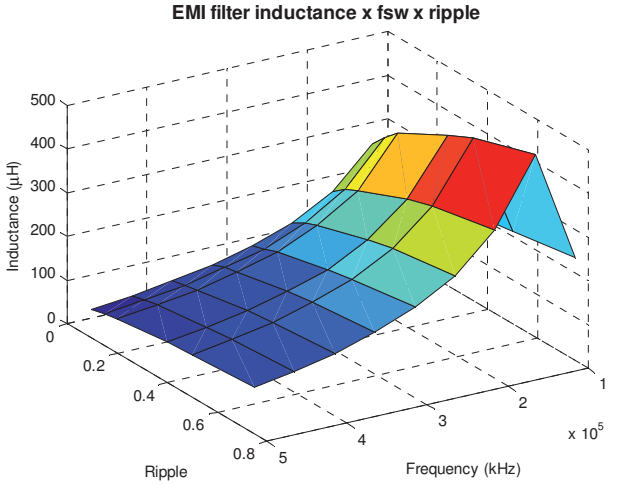

Figure 7 EMI filter inductance (µH) versus ripple and switching frequency (kHz): 2-stage LC

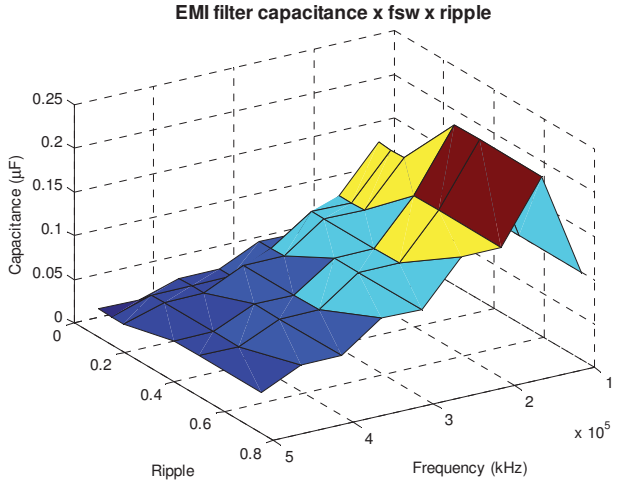

Figure 8 EMI filter capacitance (µF) versus ripple and switching frequency (kHz): 2-stage LC

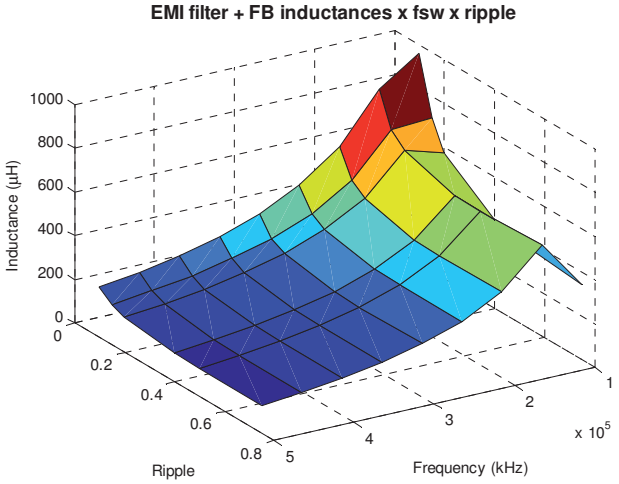

Figure 9 Power filter + EMI filter inductance (µH) versus ripple and switching frequency (kHz)

ISBN 978-3-8007-4171-7

4 Overall losses

4.1 Semiconductors losses

The commutation losses are linearly proportional to the switching frequency; however they can also be slightly influenced by higher current ripple due to the higher peak by the switch turn-off, depending on the semiconductor technology.
Extra losses from the free-wheeling diodes can become more relevant as the dead time-switching period ratio increases.
The power filter inductor reduction has an impact on the RMS value of the current flowing through the switches, which increases the conduction losses proportionally to the RMS current square.

4.2 Magnetic losses

Table 1 shows the data of two different inverter output chokes. Both chokes were built with the same foil winding and core material.

Core	**PQ50**	**PM62**
Material	N27	N27
Foil Winding	24x0.1mm	24x0.1mm
L (µH)	200	400
Rdc (mΩ)	23	33
Size (cm³)	80	150

Table 1 Inverter output chokes

The calculated winding losses for both chokes are depicted in Fig. 10. Winding losses comprise AC (skin effect in windings) and RMS losses, which appear to be dominant. Even though the HF AC resistance is significantly increasing with the frequency, there is a reduction of the current ripple, as the same inductance is considered. As a result, the AC winding losses related to the skin effect have only a very limited influence on the winding losses.

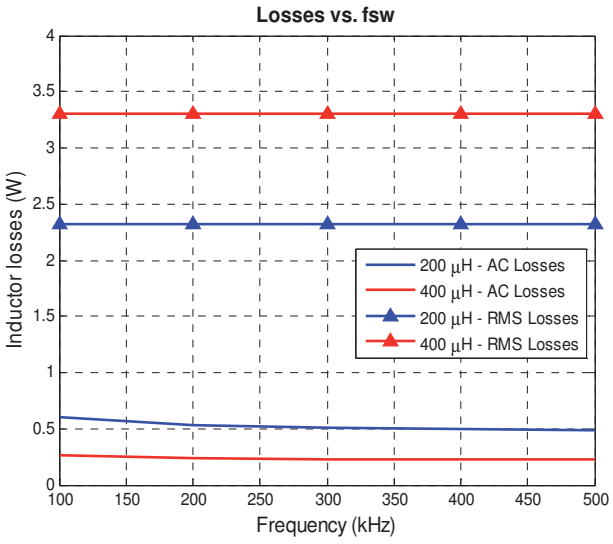

Figure 10 Winding losses versus switching frequency

The frequency dependency of the core losses (Fig. 11) is more significant. If constant inductance value is assumed, the induction (current ripple) decreases with higher frequency. The impact of the reduced induction on the core losses is more dominant than the frequency increase, leading to lesser losses as the frequency increases.
If the choke is stressed with high induction values, the total losses can increase significant at lower switching frequencies. On the other hand, the operation at high switching frequencies and low induction can decrease the total losses.
Furthermore, the reduction of the inductance value can decrease the component volume and the RMS power losses, which can also lead to lower magnetic losses at higher frequencies [8].

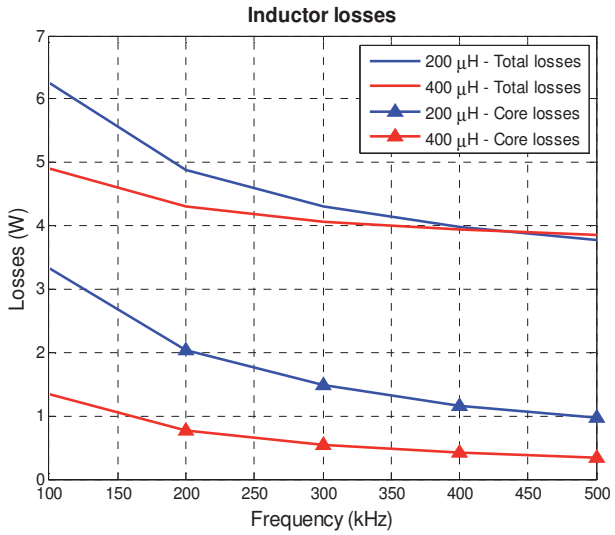

Figure 11 Inductor losses versus switching frequency

5 EMI measurements

In order to observe the influence of different inductances, EMI measurements have been performed with a LISN (HM6050-2) and Spectrum analyser (HMS-X), both from Hameg, and are shown in the following figures.
Figure 12 shows an EMI measurement of peak signal in order to compare two different power inductor values (blue: 200 µH; green: 400 µH).
Figure 13 is a comparison between the case without filtering (blue, L_{FB} = 200 µH) and a case where a filter structure has been implemented (red). Even though a clear attenuation gain is observed for the higher harmonics, the filter loses its characteristic after a few MHz, even leading to a worse EMI behaviour. This is caused by parasitic component impedances and parasitic mutual inductances between different components.

6 Discussion

One of the main goals of this paper is the discussion of the minimization possibility by increasing the switching frequency. It is clear that the power filters can be lighter and more cost-effective than nowadays, where the EMI

ISBN 978-3-8007-4171-7

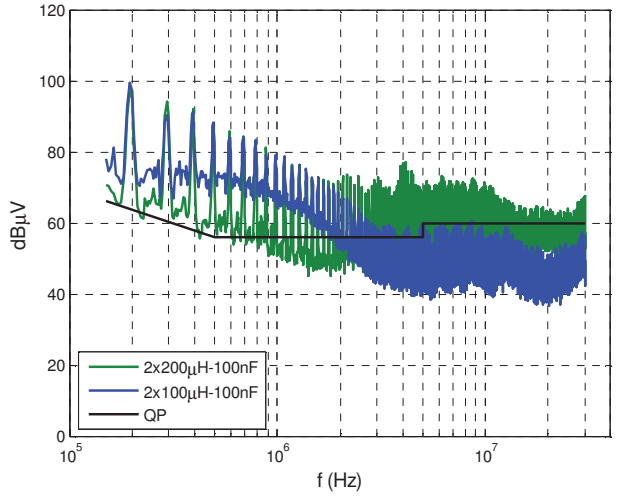

Figure 12 EMI measurement: power filter comparison and control capacitors, without additional filtering

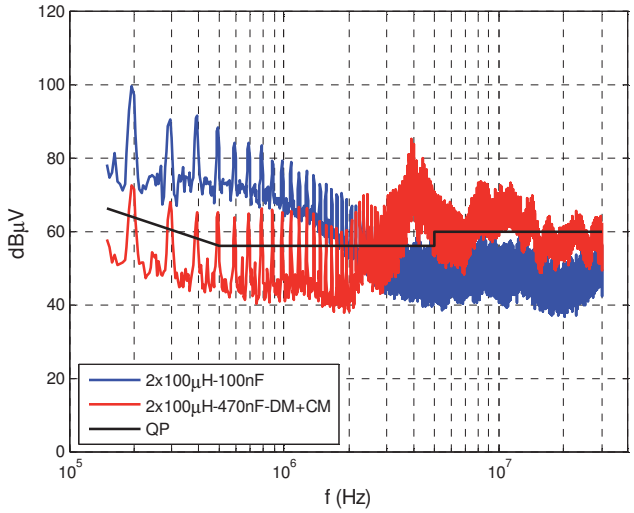

Figure 13 EMI measurement: comparison with and without EMI filter

filter expenditure must be taken into account for a proper analysis.

The attenuation provided by the large power filter inductors at the state-of-the-art lower frequency inverters (~20 kHz) is summed together with the EMI filter attenuation, leading to a smoother EMI standard-compliance.

With the cost reduction target, this attenuation from the large power filters is “not available” anymore, making the filter structure much more difficult and complicated as before.

The filter components have to be able to provide the same or higher attenuation at higher frequencies. Even though there are some strategies for magnetic components, as coreless approaches, the capacitors needed for EMI filters must be safety-compliant, which means they have more parasitic inductances leading to lower resonance frequency, and cause poor performance at high frequencies (MHz).

The combination of small power filter inductors, and consequently high current ripple, with parasitic inductances from the filter capacitors can lead to a more relevant coupling effect. As a result, the power filter inductance would have a practical value lower than designed due to the mutual inductance and the parasitic inductance from the X-capacitor would be increased.

Decoupling of filtering components or stages can be reached by shielding and PCB layout improvements.

7 Conclusion

In this paper, system compaction regarding filtering components has been analysed based on a grid-connected full-bridge inverter. It has been proven that a current ripple increase on the power filter may not minimize the overall system volume, as it could even make it larger due to the necessary EMI filtering to be standard-compliant.

As the switching frequency increases towards the EMI-standards range, a step on the filter components values has been seen at 150 kHz. Around 350 kHz the overall inductance value reduction reaches a point where the losses will define the operation frequency and ripple.

Power filter losses tend to decrease with the switching frequency increase for the same inductance value. Low induction (current ripple) at frequencies below 400 kHz has been proven to be an effective strategy to reduce the magnetic losses. At higher frequencies, the RMS losses play an important role as the minimum losses value.

The operation of the output chokes at high switching frequencies may enable the possibility of lowering the total inductor losses, if the induction is kept low. Small inductance values can potentially decrease RMS losses and therefore total losses, too.

By increasing the switching frequency, the EMI filter design becomes more complex, because of the non-linearity of magnetic components besides parasitic inductances from X and Y capacitors. It has been experimentally verified a strong influence of the components self-resonance and coupling effects.

Therefore, a trade-off between power and EMI filter components is required, in order to fulfil the main target of higher power density. From 350 kHz up to 500 kHz, a nearly constant total inductance value for every current ripple is required, indicating the minimization has reached a limit. The exact operation point will be defined by losses as well as by the magnetic components high frequency performance.

Although not the focus of this paper, further research shall be invested on semiconductor losses deeper investigation, as they may vary with the considered technology.

8 Acknowledgements

This work was developed inside the scope of the project E²COGaN, funded by ENIAC Joint Undertaking and German Ministry of Education and Research.

ISBN 978-3-8007-4171-7

9 References

[1] Araújo, S., Kleeb, T., Zacharias, P. “High switching speeds and loss reduction: prospects with Si, SiC and GaN and limitations at device, packaging and application level”. PCIM Europe 2013, Nuremberg, Germany.

[2] Mitova, R., Ghosh, R., Mhaskar, U., Klikic, D., Wang, M., Dentella, A. “Investigations on 600-V GaN HEMT and GaN diode for power converter applications”. IEEE Transactions on Power Electronics, vol. 29, No. 5, May 2014.

[3] Araújo, S., Kazanbas, Zacharias, P., Henze, N., Kirchhof, J. “Considerations on switching losses and electromagnetic compatibility (EMC) of innovative semiconductor technologies”. PCIM Europe 2010, Nuremberg, Germany.

[4] Boroyevich, D., Zhang, X., Bishinoi, H., Mattavelli, P., Wang, F. “Conducted EMI and systems integration”. CIPS 2014, Nuremberg, Germany.

[5] Raggl, K., Nussbaumer, T., Kolar, J. W. “Guideline for a simplified differential-mode EMI filter design”. IEEE Transactions on Industrial Electronics, vol. 57, No. 3, March 2010.

[6] Kim, H., Kim, K.-H. “Filter design for grid connected PV inverters”. ICSET 2008, Singapore.

[7] Ozenbaugh, R.L., Pullen, T.M. “EMI filter design”, 3rd edition, CRC Press, USA, 2012.

[8] Kleeb, T., Araújo, S., Zacharias, P. “Size and performance optimization of filter inductors for highly efficient and compact power conversion circuits”. EPE 2013, Lille, France.

ISBN 978-3-8007-4171-7